Fatigue & Fracture of Engineering Materials & Structures

doi: 10.1111/j.1460-2695.2008.01231.x

Comparison of the modified three-rail shear test and the $[(+45°,-45°)]_{ns}$ tensile test for pure shear fatigue loading of carbon fabric thermoplastics

I. DE BAERE, W. VAN PAEPEGEM and J. DEGRIECK

Department of Mechanical Construction and Production, Faculty of Engineering, Ghent University. Sint-Pietersnieuwstraat 41, B-9000 Gent, Belgium

Received in final form 18 March 2008

ABSTRACT The (three)-rail shear test is rarely considered for testing of fibre-reinforced composites under pure shear fatigue loading conditions because of all experimental difficulties. However, in this article, a carbon fabric-reinforced PPS is tested using a modified three-rail shear test setup. The results are compared with $[(+45°,-45°)]_{4s}$ tensile tests with good correspondence. All fatigue experiments were done with $R = 0$ and the influence of maximum shear stress and frequency is investigated. It can be concluded that an increase in maximum shear stress decreases fatigue lifetime, whereas an increase in frequency increases the lifetime. Before failure, a sudden increase in both temperature and permanent deformation could be detected. Creep tests yielded that the occurring deformation is mainly due to the fatigue loading, rather than due to creep phenomena.

Keywords composites; thermoplastic; three-rail shear; $[(+45°,-45°)]_{4s}$ tensile tests.

NOMENCLATURE

E_{11} Stiffness of the composite in the warp (0°) direction
E_{22} Stiffness of the composite in the weft (90°) direction
F Measured force obtained from the tensile machine
G_{12} Shear stiffness of the composite
h Height of the three-rail shear specimen
S_T Ultimate shear strength of the composite
t Thickness of the specimen (both $[(+45°,-45°)]_{4s}$ tensile as three-rail shear specimen)
w width of the $[(+45°,-45°)]_{4s}$ tensile specimen
X_T Ultimate tensile strength of the composite
Y_T Ultimate compressive strength of the composite
ε_i Strain obtained from strain gauge i in the three-rail shear test
ε_{xx} Longitudinal strain in the $[(+45°,-45°)]_{4s}$ tensile test
ε_{yy} Transverse strain in the $[(+45°,-45°)]_{4s}$ tensile test
$\varepsilon_{11}{}^{ult}$ Ultimate strain in the warp (0°) direction
$\varepsilon_{22}{}^{ult}$ Ultimate strain in the weft (90°) direction
γ_{12} Shear strain
ν_{12} Poisson's ratio of the composite
τ_{12} Shear stress

INTRODUCTION

If one wantsto study the in-plane shear behaviour of a composite, a large number of different experimental setups are available.[1,2] Typical examples are the $[+45°/-45°]_{ns}$ tensile test,[3–8] the 10° off-axis test,[8–11] the Iosipescu test,[1,9,10,12] the two- and three-rail shear test,[13–16] torsion of a rod[17] and torsion of thin-walled tubes.[18–21]

From all these tests mentioned above, the most universal method used for the determination of both in-plane shear modulus and shear strength is torsion of a thin-walled

Correspondence: I. De Baere. E-mail: Ives.DeBaere@UGent.be

tube[1] and it produces the most desired state of shear stress, free of edge effects.[16] However, this method also has some disadvantages: (i) it is rather expensive, because it requires a tension–torsion machine with specialized gripping; (ii) it cannot determine the shear characteristics of flat products, fabricated by pressing or contact moulding and (iii) the tubes required for this test are not easily fabricated.

A less expensive test is the $[+45°/-45°]_{ns}$ tensile test, because it does not require any specialized fixtures. On the other hand, these experiments are very sensitive to edge effects due to the $[+45°/-45°]$ lay-up.[16] For the 10° off-axis tests, oblique end tabs are required.[8–11]

The rail shear test positions itself somewhat in the middle. It does not require a sophisticated apparatus like the torsion setup and it induces a stress state which does not differ a lot from pure shear. Furthermore, it requires flat specimens with limited preparation.

If fatigue loading conditions are required, then the rail shear test is only rarely considered.[16] The favourite test setup remains the torsion of thin-walled tubes, despite its disadvantages, and it is sometimes combined with tension or bending in biaxial fatigue.[18–21] The $[+45°/-45°]_{ns}$ test is also used[3] for fatigue research.

The rail shear test, both two-rail and three-rail, as described in the '*ASTM D 4255/D 4255M The standard test method for in-plane shear properties of polymer matrix composite materials by the rail shear method*' has one large disadvantage: it requires the drilling of holes through the specimen, so that the clamps can be bolted to the specimen. Drilling in composites should be avoided because it nearly always causes damage to the composite and it may cause stress concentrations around the holes.[14] Furthermore, the preparation of the specimen takes more time. Hussain and Adams tried to remediate these drawbacks with a new design for the two-rail shear test.[14,15] This design no longer requires holes in the specimen. However, in these articles, fatigue was not considered.

Lessard *et al*.[16] did use the three-rail shear setup for fatigue testing, but they did not discuss any fatigue results in their article. Furthermore, they studied a unidirectionally reinforced epoxy.

The authors have already presented a modification for the three-rail shear fixture, which no longer requires holes through the specimen and is suited for fatigue testing.[22] In this article, this setup is used to test a carbon fabric-reinforced thermoplastic, namely polyphenylene sulphide (PPS), under in-plane fatigue loading conditions. The results obtained from these experiments are compared with results from the $[(+45°,-45°)]_{4s}$ tensile fatigue test. To the authors' best knowledge, such a comparison has not been presented before, because no rail shear fatigue data have ever been published. All tests were performed with a stress ratio equal to zero and the influence of both the loading frequency and maximum shear stress was examined. Creep tests were also performed with both setups to verify whether the detected permanent deformation was due to creep phenomena or to fatigue damage.

In the next section, the used material and methods are presented. Then, the three-rail shear tests are discussed. This is followed by the $[(+45°,-45°)]_{4s}$ fatigue experiments, and finally some conclusions are drawn.

MATERIALS AND METHODS

Composite material

The material under study was a carbon fibre-reinforced PPS, called CETEX. This material is supplied to us by TenCate. The fibre type is the carbon fibre T300J 3K and the weaving pattern is a 5-harness satin weave with a mass per surface unit of 286 g/m^2. The 5-harness satin weave is fabric with high strength in both directions and excellent bending properties.

The carbon PPS plates were hot pressed, only one stacking sequence was used for this study, namely a $[(0°,90°)]_{4s}$, where (0°,90°) represents one layer of fabric.

The in-plane elastic properties of the individual carbon PPS lamina were determined by the dynamic modulus identification method as described in Ref. [23] and are listed in Table 1.

The tensile strength properties were determined at the Technical University of Delft and are listed in Table 2.

Equipment

All tensile tests were performed on a servo-hydraulic INSTRON 1342 tensile testing machine with a Fast-Track 8800 digital controller and a load cell of ±100 kN.

Table 1
In-plane elastic properties of the individual carbon/PPS lamina (dynamic modulus identification method)

E_{11}	56.0	GPa
E_{22}	57.0	GPa
ν_{12}	0.033	-
G_{12}	4.175	GPa

Table 2
Tensile strength properties of the individual carbon/PPS lamina (mechanical testing at TUDelft)

X_T	617.0	MPa
ε_{11}^{ult}	0.011	-
Y_T	754.0	MPa
ε_{22}^{ult}	0.013	-
S_T	110.0	MPa

The quasi-static tests were displacement-controlled with a speed of 2 mm/min.

For the registration of the tensile data, a combination of a National Instruments DAQpad 6052E for fireWire, IEEE 1394 and the SCB-68 pin shielded connecter were used. The load, displacement and strain, given by the FastTrack controller, were sampled on the same time basis.

EXPERIMENTAL PROCEDURE

Three-rail shear tests

These tests were done according to the ASTM D4255/D4255M '*standard test method for in-plane shear properties of polymer matrix composite materials by the rail shear method*' but under fatigue loading conditions. Furthermore, the modified three-rail shear design, as documented in Ref. [22] is used. This design is illustrated in Fig. 1 and differs from the standard setup because the new design no longer requires bolts mounted through the specimen. The gripping is based on friction and geometrical clamping and the bolts are used to press a load transfer plate against the specimen, generating the normal force, necessary for the frictional clamping.

Fig. 1 The modified three-rail shear setup, as presented in Ref. [22].

The dimensions of the used specimen are given in Fig. 2.

The quasi-static tests were done in a displacement-controlled manner with a displacement speed of 1 mm/min, during which the force F, the strains ε_i, $i = 1,2,3,4$ and the temperature were recorded. With these values, the shear stress and strain can be calculated as

$$\tau_{12} = \frac{1}{2}\frac{F}{t\,h} \qquad \gamma_{12} = |\varepsilon_i - \varepsilon_j|, \tag{1}$$

where h is the height of the specimen and t the thickness; (i, j) is either (1, 2) or (3,4) with respect to the numbering of the strain gauges in Fig. 2.

The fatigue experiments were done in a load-controlled manner and force, displacement and temperature were registered. Because of the large deformations, strain gauges were not considered, because they de-bond after a few dozen cycles. As such, the displacement is chosen as parameter for information about the deformed state because there is a relationship between the shear strain and the displacement, because of the geometrical clamping of the grips. The latter was also shown in Ref. [22].

$[(+45°, -45°)]_{4s}$ experiments

The purpose of these tests is to verify if the results obtained from the modified three-rail shear setup can also be reproduced by a different kind of experiment, which also induces an in-plane shear stress state. These experiments were done according to the '*ASTM D3479/D3479M-96 (2002) standard test method tension–tension fatigue of polymer matrix composite materials*' and the '*ASTM D3518-76 standard practice for in-plane shear stress–strain response of unidirectional reinforced plastics*'. The dimensions of the used coupons are shown in Fig. 3.

The quasi-static tensile tests were done in a displacement-controlled manner with a displacement speed of 2 mm/min, during which the force F, the longitudinal and transverse strains, ε_{xx} and ε_{yy}, and the temperature were recorded. With these values, the shear stress τ_{12} and shear strain γ_{12} can be calculated as

$$\tau_{12} = \frac{1}{2}\frac{F}{wt} \qquad \gamma_{12} = \varepsilon_{xx} - \varepsilon_{yy}| \tag{2}$$

where w is the width of the specimen and t is the thickness.

The transverse strain was measured using a strain gauge and the longitudinal strain was measured using the

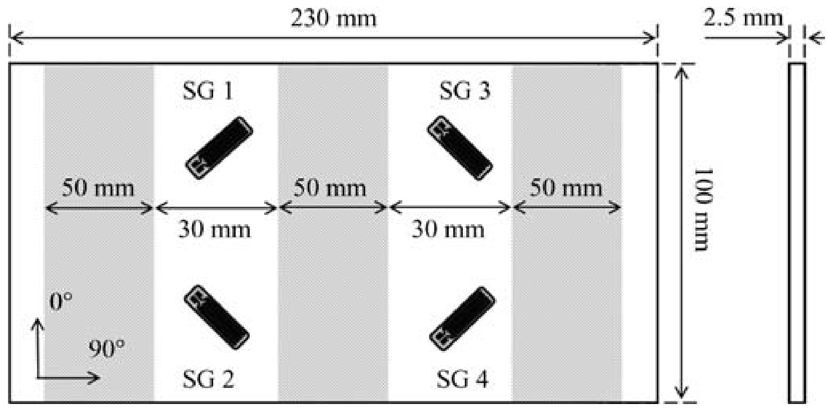

Fig. 2 Dimensions of the used $[(0°, 90°)]_{4s}$ three-rail shear specimen. The location of the strain gauges, as well as the clamps, is also illustrated.

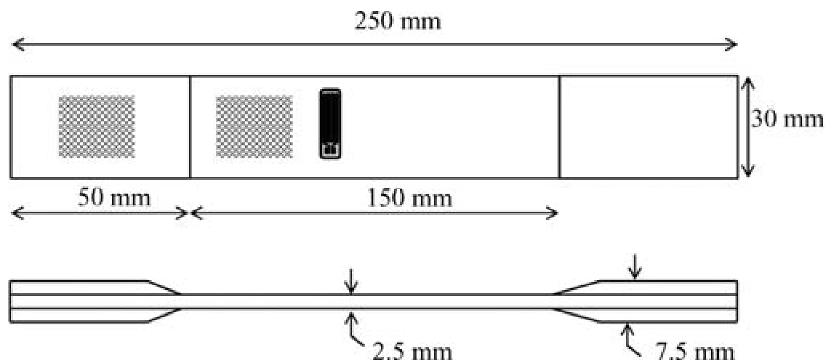

Fig. 3 Dimensions of the used $[(+45°,-45°)]_{4s}$ tensile coupon, equipped with chamfered tabs of $[(+45°,-45°)]_{4s}$ carbon PPS.

extensometer. The fatigue experiments were done in a load-controlled manner; because of the large deformations, strain gauges were not considered as they would de-bond after a few dozen cycles. The longitudinal strain was measured with the extensometer, but as there are no data for the transverse strain, the shear strain cannot be calculated. Of course, load, displacement and temperature were also registered.

DISCUSSION

Quasi-static tests

The purpose of these tests is to estimate which values of the maximum load level during the fatigue experiments would be interesting. Some results from quasi-static tests are given in Fig. 4. Since two curves can be derived from each rail shear test, one from each instrumented loaded zone, there should be six curves for three specimens. However, in Fig. 4, only the curves from the strain gauges which lasted the longest are given; the tests were stopped once all strain gauges de-bonded or saturated which means that the maximum value of the shear stress and strain in Fig. 4 does not correspond with failure. After saturation or failure of the gauges, the test was stopped so the possibility for non-destructive evaluation of the specimens remained an option.

With respect to the $[(+45°,-45°)]_{4s}$ experiments, two quasi-static experiments, N1 and M3, are shown in Fig. 4. The curve is only depicted until the transverse strain gauge either saturated, which was the case for M3, or de-bonded, which happened for N1. The failure stresses were 105.4 and 105.3 MPa for N1 and M3, respectively. These values show good correspondence with the value given in Table 2.

It should be noticed that the results from these quasi-static tests are very reproducible and that the calculated stiffness corresponds very well with the value obtained with the dynamic modulus identification method (Table 1). During the experiments, no temperature increase was measured.

From these results, a maximum stress level between 30 and 50 MPa for the fatigue tests should give interesting results. Lower than 30 MPa, there is only very limited nonlinear behaviour and beyond 50 MPa it is expected that the specimen would fail after a few dozen cycles.

Fatigue loading conditions

Because the objective is to compare the results of the three-rail shear test with the $[(+45°,-45°)]_{4s}$ tensile tests, all fatigue experiments were done with a shear stress ratio *R* equal to 0, meaning that the shear stress varies between 0 and a certain maximum value. For the $[(+45°,-45°)]_{4s}$ tensile test, it would be rather difficult to have negative

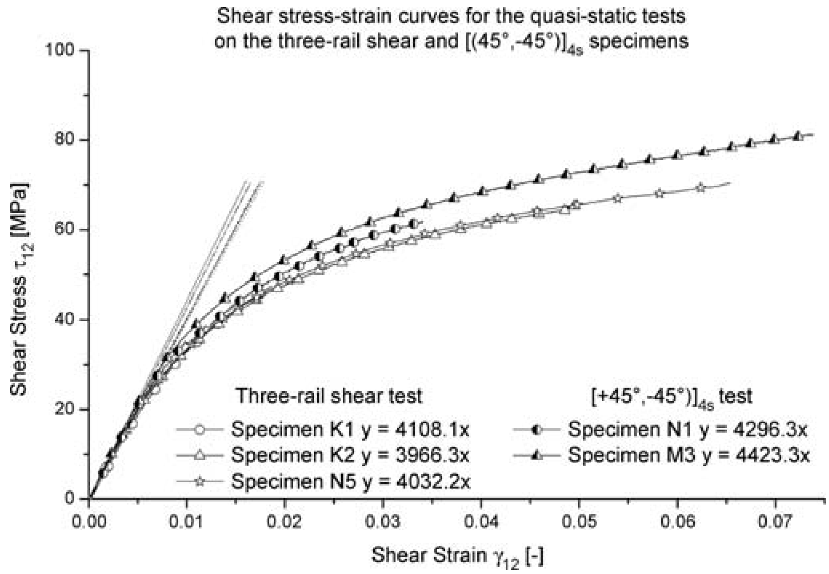

Fig. 4 Evolution of the shear stress as a function of the shear strain for the quasi-static experiments.

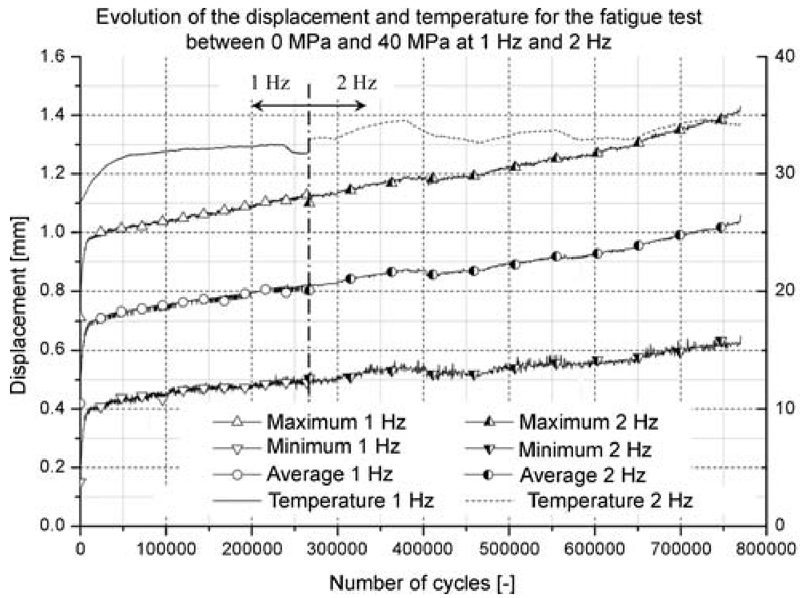

Fig. 5 Maximum, minimum and mean value of the displacement as a function of the number of cycles for a 0–40 MPa fatigue test at a combined frequency of 1 and 2 Hz.

shear stresses, because this would mean that compressive tests should be performed, with the corresponding difficulties with buckling.

During the fatigue experiments, every five minutes five fatigue cycles were registered and from these signals, the maximum, minimum and average values were calculated and stored.

A first rail shear experiment was done at 1 Hz with a maximum load of 40 MPa, which is halfway through the range suggested in the previous paragraph. Because the test was load controlled, an increase in the displacement amplitude corresponds with shear stiffness degradation. While monitoring the experiment, it was noticed that the permanent deformation and stiffness degradation were less than expected and no temperature increase occurred, so after 250000 cycles, the frequency was increased to 2 Hz. The results of this experiment are shown in Fig. 5. After 770000 cycles, the test was stopped.

The temperature tends to be slightly higher for 2 Hz than for 1 Hz. Therefore, the next rail shear test was done between 0 and 40 MPa at 2 Hz until failure. Fig. 6 illustrates the run-in of the experiment and Fig. 7 shows the fatigue data. It should be noted that already some permanent deformation occurs during the run-in, followed by a steady-state regime. That is also the reason why the minimum of the displacement during the fatigue test does not start at 0 in Fig. 7. It can also be noticed that the evolution of the displacement does not have the expected sinusoidal evolution with increasing amplitude. The test was load-controlled with a sinusoidal evolution and due

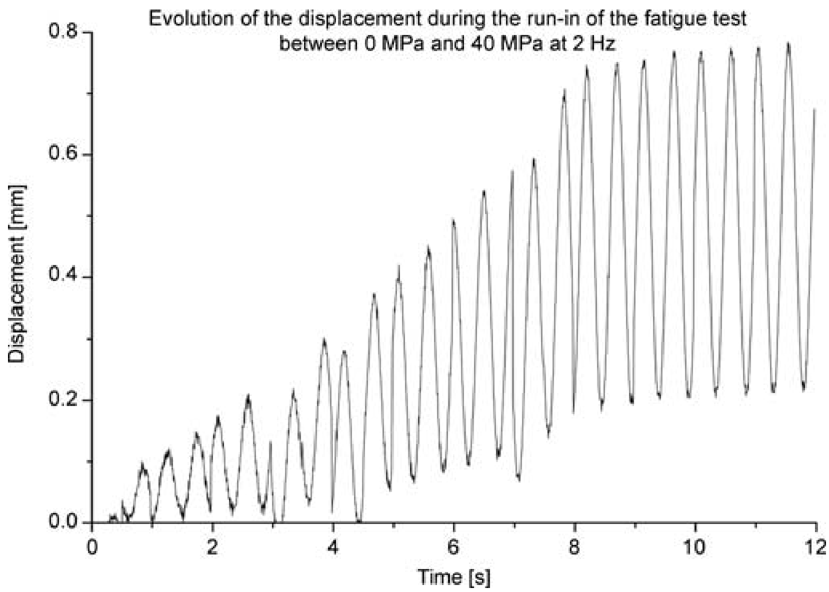

Fig. 6 Displacement as a function of time during the run-in of the 0–40 MPa, 2 Hz fatigue test.

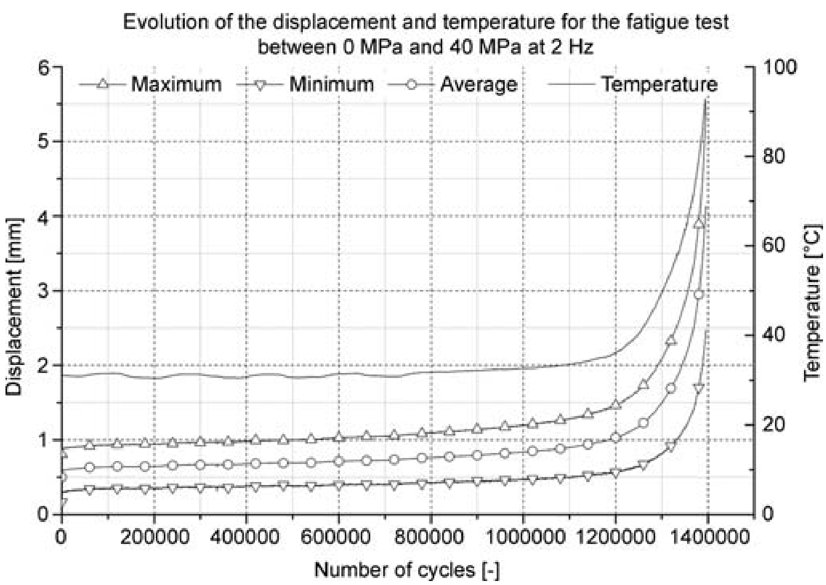

Fig. 7 Maximum, minimum and mean value of the displacement as a function of the number of cycles for a 0–40 MPa fatigue test at 2 Hz.

to stick slip, the corresponding displacement differs a little.

The test was stopped after 1400000 cycles because the temperature had already exceeded the glass transition temperature of the matrix, which is 90 °C. From Fig. 7, it can be seen that after the run-in there is a gradual increase in permanent deformation and stiffness degradation, until about 1200000 cycles. Until that time, the temperature remains constant. Then, there is a sudden increase in both temperature and permanent deformation. This can be explained as follows. During the first 1200000 cycles, damage grows in the material, with little effect on the stiffness. Probably the fibre–matrix interface deteriorates. Once there is sufficient damage to this interface, the fibres start to slide inside the matrix under the influence of the shear load, causing heating of the matrix, with softening of the matrix as a result. This, however, causes more deterioration of the fibre–matrix interface, so that even more sliding and heating occur. This process ends with final failure. The heating due to frictional sliding of the fibre in the matrix has also been reported in Refs [24] and [25] for fibre-reinforced ceramics and in Ref. [26] for fibre-reinforced polymers.

Due to the long duration of this experiment, these loading conditions were not implemented for the $[(+45°,-45°)]_{4s}$ experiments.

The following experiment was done between 0 and 45 MPa at 2 Hz to assess the influence of maximum load level. The run-in gave similar results as for the 0–40 MPa test, so it is not shown. Figure 8 depicts two of these experiments for the three-rail shear setup.

Again, a similar evolution as for the 0–40 MPa test can be seen, although the initiation of the large stiffness decrease and sudden temperature increase happens a lot earlier. For these tests, the sudden jump happens around 140000 cycles for N3 and around 310000 cycles for M1. This is five to 10 times lower than for the 0–40 MPa at the same frequency. It should, however, be noted that the increase in permanent deformation is much more sudden for N3 than for M1. For the latter, the sudden jump is preceded by a gradual increase in permanent deformation and stiffness degradation, which both start around 150000 cycles. The latter is also the point in time where the temperature starts increasing. The sudden drop in temperature around 300000 cycles for M1 was due to a loss of contact of the thermocouple, because of the large deformations. The thermocouple was re-attached soon afterwards.

In Fig. 9, the fracture of this specimen is shown. Although the failure started near the clamped edges, where stress concentrations exist, final failure occurred in the centre of the specimen, under shear loading conditions.

With respect to the $[(+45°,-45°)]_{4s}$ experiments, the following remarks must be made. For comparison of the results with the rail shear tests, the evolution of the displacement is illustrated. For each experiment, it was verified that no slipping in the grips occurred. Also, the evolution of both temperature and displacement is only considered until there is a significant temperature increase and stiffness degradation. Afterwards, a new regime reinstates itself, which is discussed at the end of this paragraph.

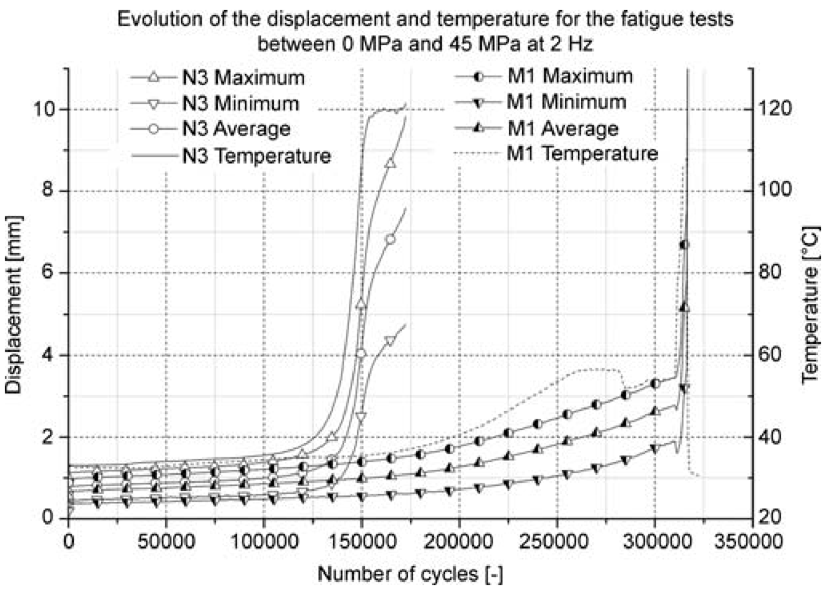

Fig. 8 Maximum, minimum and mean value of the displacement as a function of the number of cycles for a 0–45 MPa fatigue test at 2 Hz; three-rail shear experiments.

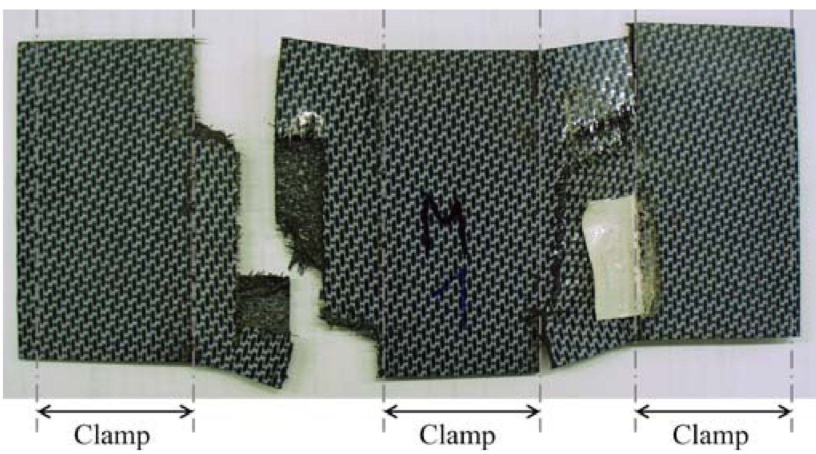

Fig. 9 Illustration of the failure of specimen M1.

Fig. 10 Deformed (top) and undeformed (bottom) $[(+45°,-45°)]_{4s}$ specimen.

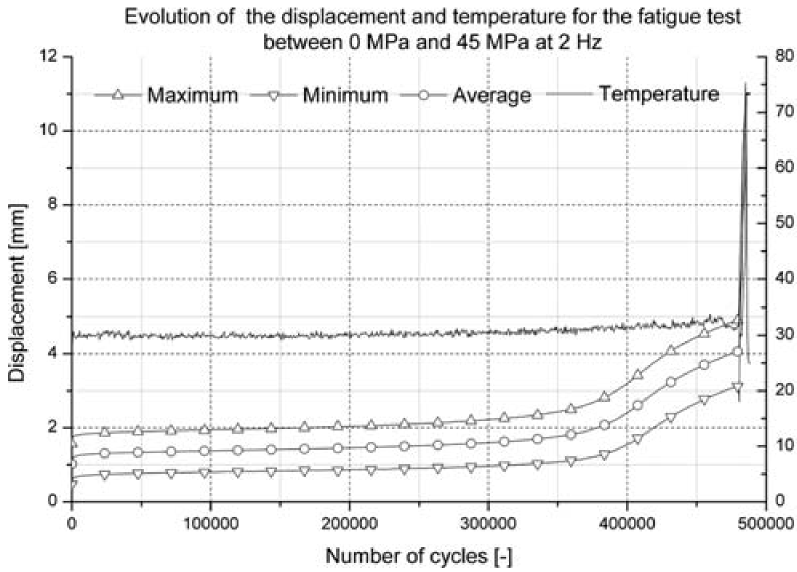

Fig. 11 Maximum, minimum and mean value of the displacement as a function of the number of cycles for a 0–45 MPa tensile fatigue test at 2 Hz; $[(+45°,-45°)]_{4s}$ experiment.

Moreover, the specimens tend to deform into a 'dog bone' like shape. This deformation was most apparent for the highest stress range and frequency, which is illustrated in Fig. 10, where the specimen N2, on which a 0–50 MPa, 2 Hz fatigue experiment was done, can be compared with another specimen which is still to be tested, but with the same dimensions as specimen N2 had before testing.

Figure 11 shows the corresponding results from a fatigue tensile test between 0 and 45 MPa at 2 Hz. The initiation of the increase in temperature and deformation is situated around 400000 cycles, which is higher than the 140000 and 310000 cycles found for the corresponding rail shear test.

Because of this difference in lifetime, the following experiments were conducted in the same stress range, 0–45 MPa, but at 1 Hz, to assess the influence of the frequency. The results of these experiments are shown in Fig. 12. The temperature measurement was unavailable for specimen M3, because the thermocouple de-bonded very early. Again, similar evolutions are found for the evolution of the displacement. Specimen M4 has a sudden increase in temperature and displacement after about 80000 cycles, whereas specimen M3 has a more gradual increase, starting around 100000, until there is a sudden increase at 160000 cycles. Apparently, lowering the frequency tends to decrease the lifetime. The initiation of both the increase in temperature and deformation growth occurs around 280000 cycles for the tensile test, which is again higher than for the rail shear tests.

To verify this behaviour, fatigue experiments were done at a load range of 0–50 MPa and again at 1 and 2 Hz. When examining the run-in of these experiments for the rail shear test, similar evolutions as for the 0–40 MPa@2 Hz test were found (see Fig. 6), namely a relatively large increase, followed by a steady-state regime.

Figure 13 shows the results for the rail shear tests at 2 Hz. The sudden increase for the displacement occurs around 55000 cycles for N1 and around 45000 cycles for L5. It should be noted that due to the large deformations, the thermocouple de-bonded after 59000 cycles for N1, hence the sudden drop in temperature. Furthermore, the temperatures lie lower than in the previous experiments, because the thermocouple lost contact with the specimen's surface, due to the large deformations, but still remained quite close to the surface. As such, the actual temperatures would be in the same range as for the previous tests, which means higher than the softening temperature of PPS (90 °C).

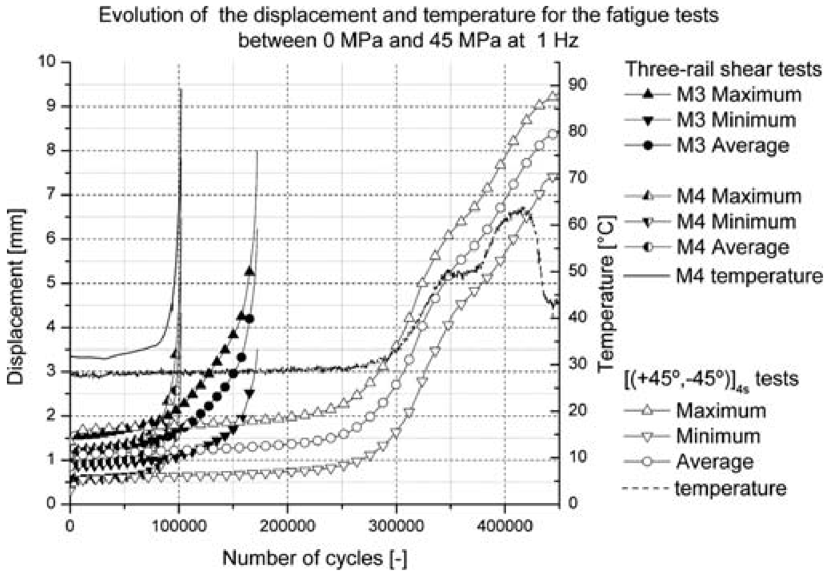

Fig. 12 Maximum, minimum and mean value of the displacement as a function of the number of cycles for a 0–45 MPa fatigue test at 1 Hz.

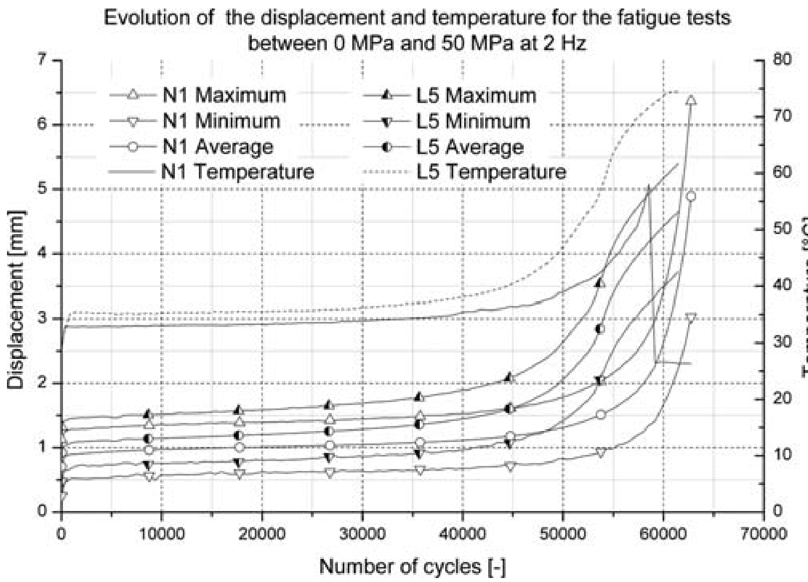

Fig. 13 Maximum, minimum and mean value of the displacement as a function of the number of cycles for a 0–50 MPa fatigue test at 2 Hz; three-rail shear experiments.

Considering the lifetime, a reduction factor of about three with respect to the 0–45 MPa@2 Hz measurements is found.

Figure 14 shows the results from two of the conducted 0–50 MPa@2 Hz tensile experiments. It can be remarked that the behaviour is very similar to the three-rail shear tests. The sudden jump occurs at 70000 cycles for N2 and at 125000 cycles for N5, which is higher than the corresponding rail shear tests, where the jump occurred at 45000 and 55000 cycles. However, an increase in frequency again tends to yield an increase in lifetime, corresponding with the rail shear test.

Figure 15 illustrates the results from the 0–50 MPa@1 Hz experiment for both the rail shear and tensile test. Unfortunately, the temperature measurement was not successful for the rail shear test because of the de-bonding of the thermocouple. The sudden increase in displacement occurs after about 27500 cycles for the rail shear test and at 45000 cycles for the tensile test. Both are indeed lower than for the corresponding experiment at 2 Hz, but again the lifetime is higher for the tensile test than for the three-rail shear experiment.

Finally, the entire measured evolution of the displacement for the 0–50 MPa@2 Hz on the $[(+45^{\circ},-45^{\circ})]_{4s}$ specimen N2 (see Fig. 14) is given in Fig. 16. As can be seen, a different behaviour manifests itself after the rise in temperature and decrease in stiffness.

The evolution of both displacement and temperature is very similar to the three-rail shear test until the point of

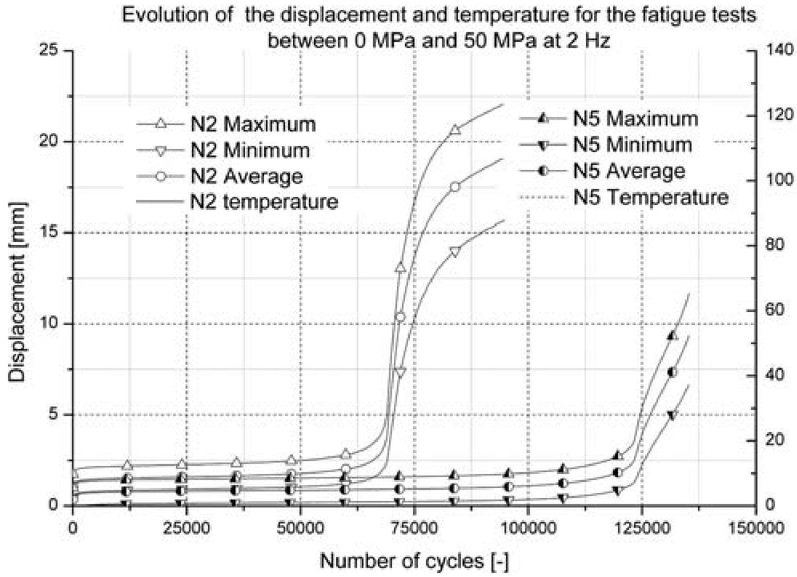

Fig. 14 Maximum, minimum and mean value of the displacement as a function of the number of cycles for a 0–50 MPa tensile fatigue test at 2 Hz; $[(+45°,-45°)]_{4s}$ experiments.

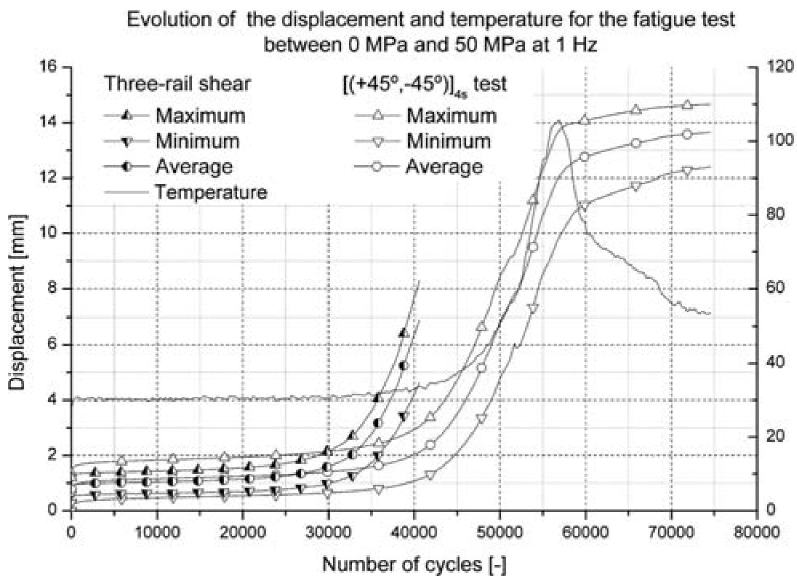

Fig. 15 Maximum, minimum and mean value of the displacement as a function of the number of cycles for a 0–50 MPa fatigue test at 1 Hz.

the sudden rise in temperature and deformation, which occurs here at about 60000 cycles. For the three-rail shear test, the specimen failed soon after the rise in temperature, but for the $[(+45°,-45°)]_{4s}$ tensile test, a new regime initiates. After the sudden rise in temperature, which again exceeds the softening temperature of the matrix, the specimen cools down and no further increase in displacement or stiffness degradation manifests itself. This can be explained by re-observing the images of the specimen after the test (Fig. 10).

This 'dog bone' like shape arose during the heating of the specimen. Because of the softening of the matrix, the fibres were able to realign considerably with respect to the loading direction. This can be seen in a detailed image of specimen N2 (see Fig. 17).

As such, a new load distribution occurs, with less shear load and more load along the fibres and Eq. (2) for the shear stress and strain is no longer valid. Therefore, after the sudden rise in temperature and displacement, no more increase in stiffness degradation or deformation occurs, because the specimen is now loaded more along the fibres.

During the increase in temperature, the force–displacement hysteresis loops become much wider, as illustrated in Fig. 18, indicating that a lot of energy is dissipated, both in damage and, of course, in the heating of the specimen.

Furthermore, it must be remarked that the narrowing of the specimen to a 'dog bone' like shape, as illustrated in Fig. 10, does not happen in a uniform manner over the entire specimen, but starts near the clamped ends and

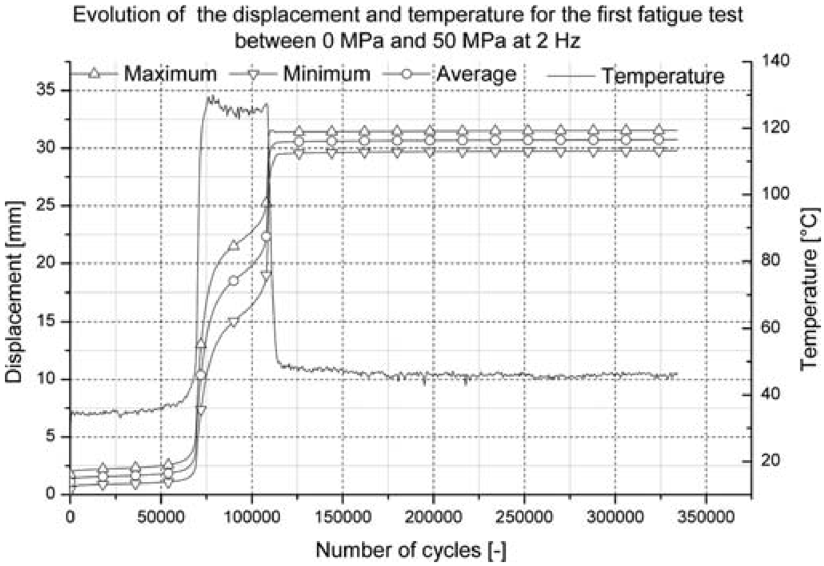

Fig. 16 Maximum, minimum and mean value of the displacement as a function of the number of cycles for the preliminary 0–50 MPa tensile fatigue test at 2 Hz.

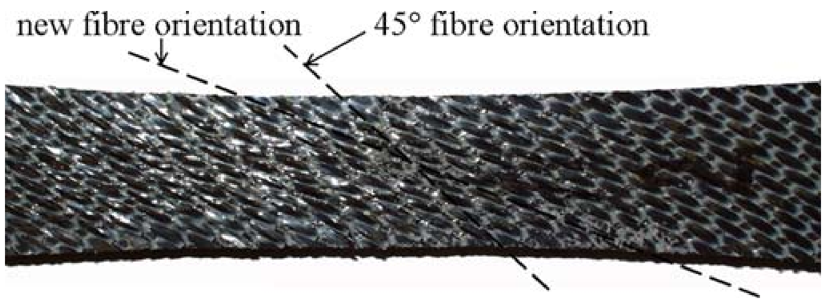

Fig. 17 Illustration of the change in fibre orientation due to the softening of the matrix.

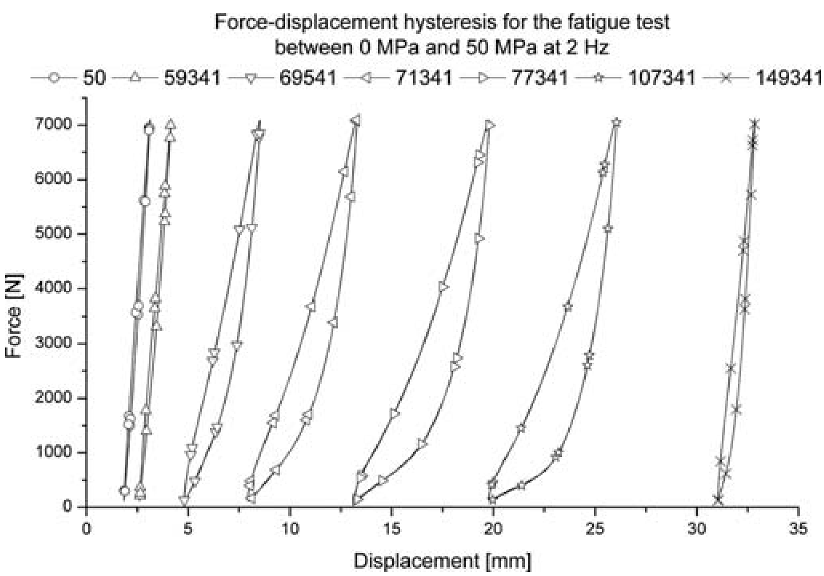

Fig. 18 Force as a function of the displacement for a few measurements of the tensile fatigue test on specimen N2.

then gradually grows along the entire specimen length. This growing of the localization of the shear strain could clearly be seen in the experiments.

In conclusion, increasing the maximum shear stress for fatigue tests with R equal to zero decreases the fatigue life, while increasing the loading frequency for a given load range seems to increase fatigue life. The fatigue life is very sensitive to the maximum shear stress at low maximum stresses; an increase from 40 to 45 MPa (for the rail shear) decreased fatigue life by a factor of 10. For higher stresses, the sensitivity is lower; an increase from 45 to 50 MPa only reduces fatigue life by a factor of about 3.

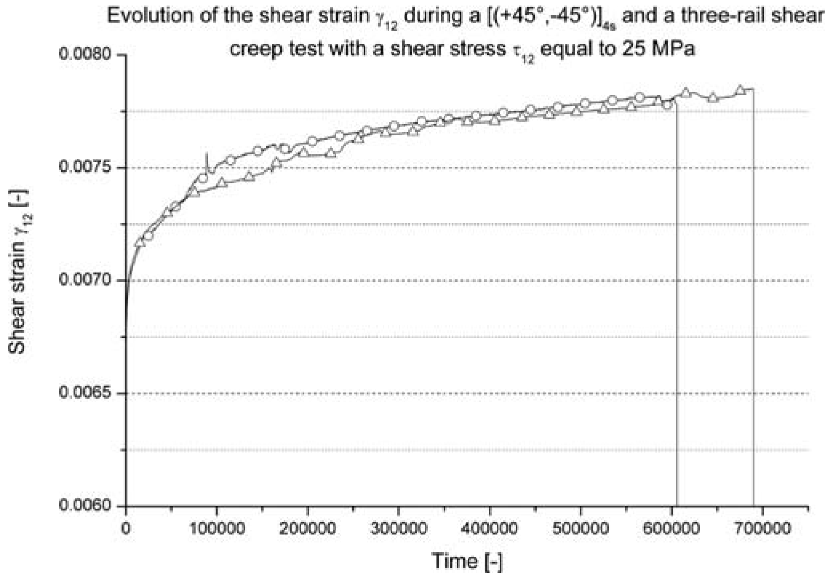

Fig. 19 Shear strain as a function of time for both the three-rail shear and the $[(+45°,-45°)]_{4s}$ creep test.

During run-in, there is firstly a relatively large increase in displacement. Then, there is some sort of steady state with a very gradual increase and finally, a sudden large increase in both temperature and displacement occurs, before failure.

With respect to the correspondence between the three-rail shear test and the $[(+45°,-45°)]_{4s}$ tests, the point in time where both the sudden temperature increase as the stiffness decrease occur is situated a little later for the tensile test than for the rail shear test. Also, after this increase, the $[(+45°,-45°)]_{4s}$ specimen does not fail, but a new regime re-instates itself, due to a re-alignment of the fibres along the loading direction, because of the softening of the matrix.

Creep testing

All fatigue experiments documented in this article were done with a stress ratio equal to zero, meaning that the force, and therefore shear stress, had a sinusoidal evolution between 0 MPa and a certain maximum value τ_{max} MPa. This, however, means that the specimen is subjected to an average loading of half of τ_{max} during the entire fatigue test. Because of the thermoplastic nature of the matrix, the matrix may suffer from creep. In this article, the fatigue life is considered to be the number of cycles at which there is a sudden increase in temperature and permanent deformation. The purpose of the creep test is to verify whether the permanent deformation during fatigue cycling until this point is the result of fatigue damage, creep damage or a combination of both. Because during fatigue cycling the temperature remains relatively stable around room temperature, the creep tests were also performed at room temperature.

A creep test was performed both with the three-rail shear test and with the $[(+45°,-45°)]_{4s}$ test and a constant shear stress of 25 MPa was applied. The latter corresponds with the fatigue tests with a maximum shear stress of 50 MPa, which are the heaviest fatigue loading conditions for this article. Both the rail shear specimen and the tensile specimen were instrumented with two strain gauges, in order to evaluate the evolution of the shear strain. The load was applied for about 700000 s, which equals 700000 cycles at 1 Hz or 1400000 cycles at 2 Hz for the three-rail shear test and for about 600000 s, corresponding with 600000 cycles for a 1 Hz test and 1200000 cycles for a 2 Hz test for the $[(+45°,-45°)]_{4s}$ specimen. The evolution of the shear strain γ_{12} for both experiments is depicted in Fig. 19. As can be seen, the absolute increase in shear strain is less than 0.0008 for both test setups. Again, the correspondence is very good.

Because the shear strain could not be registered during the fatigue experiments, only information about the displacement is available. For the three-rail shear test, an increase of only 0.05 mm over 700000 s occurred and for the $[(+45°,-45°)]_{4s}$ test, an increase of 0.05 mm was measured. Therefore, it may be concluded that the increase in displacement during the fatigue test is mainly caused by fatigue damage, because the measured increase is larger.

CONCLUSIONS

In this article, the in-plane shear fatigue behaviour of a carbon fabric-reinforced PPS has been examined by performing and comparing three-rail shear experiments with $[(+45°,-45°)]_{4s}$ tensile experiments. All experiments were done with a stress ratio equal to 0, meaning that the shear stress varied between 0 MPa and a certain maximum. For both types of experiments, the same conclusions could be drawn with respect to the frequency and the maximum shear stress: (i) increasing the maximum shear stress decreases fatigue lifetime and (ii) increasing the frequency seems to increase the fatigue lifetime. The results from both types of tests show good correspondence, although the lifetime was always higher for the $[(+45^\circ,-45^\circ)]_{4s}$ tensile test. The material behaviour itself can be described in three stages: (i) run-in of the fatigue test, where a certain amount of permanent deformation occurs without an increase in temperature; (ii) a steady-state phase, where there is a gradual increase in permanent deformation, without an increase in temperature and (iii) the end-of-life phase, where there is a sudden increase in temperature, above the softening temperature of the matrix and a sudden growth in permanent deformation.

Two final remarks should be made: (i) for the three-rail shear test, the end-of-life phase ended with failure of the specimen, whereas for the $[(+45^\circ,-45^\circ)]_{4s}$ test, a 'dog bone' like shape was formed, with re-alignment of the fibres along the loading direction; (ii) creep tests were performed to verify whether the constant growth of permanent deformation during the 'steady-state' phase was due to fatigue damage. It could be concluded that the material did creep, but the main damage occurred due to the fatigue loading conditions.

Acknowledgments

The authors are highly indebted to the university research fund BOF (Bijzonder Onderzoeksfonds UGent) for sponsoring this research and to TenCate Advanced Composites for supplying the material.

REFERENCES

1 Tarnopol'skii, Y. M., Arnautov, A. K. and Kulakov, V. L. (1999) Methods of determination of shear properties of textile composites. *Compos. Part A-Appl. Sci. Manuf.* **30**, 879–885.

2 Whitney, J. M., Daniel, I. M. and Pipes, R. B. (1984). Experimental mechanics of fiber reinforced composite materials. Chapter 4. Composite characterization. The Society for Experimental Mechanics, Connecticut, pp. 160–202.

3 Shalom, S., Harel, H. and Marom, G. (1997) Fatigue behaviour of flat filament-wound polyethylene composites. *Compos. Sci. Technol.* **57**, 1423–1427.

4 Maeda, T., Baburaj, V. and Koga, T. (1997) Evaluation of in-plane shear modulus of composite laminates using holographic interferometry. *Opt. Engng* **36**, 1942–1946.

5 Echtermeyer, A. T. (1994) Evaluation of the [±45]s inplane shear test method for composites reinforced by multiaxial fabrics. In: *ECCM-CTS 2 : Composites testing and standardisation, European Conference on composites testing and standardisation, 13–15 September 1994* (Edited by P.J. Hogg, K. Schulte and H. Wittich), Woodhead Publishing Limited, Hamburg, Germany, pp. 305–313.

6 Payan, J., Hochard, C. (2002) Damage modelling of laminated carbon/epoxy composites under static and fatigue loadings. *Int. J. Fatigue* **24**, 299–306.

7 Khashaba, U. A. (2004) In-plane shear properties of cross-ply composite laminates with different off-axis angles. *Compos. Struct.* **65**, 167–177.

8 Van Paepegem, W., De Baere, I. and Degrieck, J. (2006) Modelling the nonlinear shear stress-strain response of glass fibre-reinforced composites. Part I: Experimental results. *Compos. Sci. Technol.* **66**, 1455–1464.

9 Odegard, G. and Kumosa, M. (2000) Determination of shear strength of unidirectional composite materials with the Iosipescu and 10° off-axis shear tests. *Compos. Sci. Technol.* **60**, 2917–2943.

10 Pierron, F and Vautrin, A. (1997) New ideas on the measurement of the in-plane shear strength of unidirectional composites. *J. Compos. Mater.* **31**, 889–895.

11 Pierron, F and Vautrin, A. (1996) The 10° off-axis tensile test: a critical approach. *Compos Sci. Technol.* **56**, 483–488

12 Odom, E. M., Blackketter, D. M. and Suratno, B. R. (1994) Experimental and analytical investigation of the modified Wyoming shear-test fixture. *Exp. Mech.* **34**, 10–15.

13 Hussain, A. K. and Adams, D. F. (1999) The Wyoming-modified two-rail shear test fixture for composite materials. *J. Compos. Technol. Res.* **21**, 215–223.

14 Hussain, A. K. and Adams, D. F. (2004) Experimental evaluation of the Wyoming-modified two-rail shear test method for composite materials. *Exp. Mech.* **44**, 354–364.

15 Hussain, A. K. and Adams, D. F. (2004) Analytical evaluation of the two-rail shear test method for composite materials. *Compos. Sci. Technol.* **64**, 221–238.

16 Lessard, L. B., Eilers, O. P. and Shokrieh, M. M. (1995) Testing of in plane shear properties under fatigue loading. *J. Reinf. Plast. Compos.* **14**, 965–987.

17 Ferry, L., Perreux, D., Varchon, D. and Sicot, N. (1999) Fatigue behaviour of composite bars subjected to bending and torsion. *Compos. Sci. Technol.* **59**, 575–582.

18 El-Assal, Ahmed M. and Khashaba, U. A. (2007) Fatigue analysis of unidirectional GFRP composites under combined bending and torsional loads. *Compos. Struct.* **79**, 599–605.

19 Qi, Dongtao and Cheng, Guangxu. (2007) Fatigue behavior of filament-wound glass fiber reinforced epoxy composite tension/torsion biaxial tubes under loading. *Polym. Compos.* **28**, 116–123.

20 Kawakami, H., Fujii, T. J. and Morita, Y. (1996) Fatigue degradation and life prediction of glass fabric polymer composite under tension torsion biaxial loadings. *J. Reinf. Plast. Compos* **15**, 183–195.

21 Fujii, T and Lin, F. (1995) Fatigue behaviour of a plain-woven glass fabric laminate under tension-torsion biaxial loading. *J. Compos. Mater.* **29**, 573–590.

22 De Baere, I., Van Paepegem, W. and Degrieck, J. (2008) Design of a modified three-rail shear test for shear fatigue of composites. *Polym. Test.* **27**, 346–359.

23 De Baere, I., Van Paepegem, W., Degrieck, J., Sol, H., Van Hemelrijck, D. and Petreli, A. (2007) Comparison of different identification techniques for measurement of quasi-zero Poisson's ratio of fabric reinforced laminates. *Compos. Part A-Appl. Sci. Manuf.* **38**, 2047–2054.

24 Cho, C. D., Holmes, J. W. and Barber, J. R. (1991) Estimation of interfacial shear in ceramic composites from frictional heating measurements. *J. Am. Ceram. Soc.* **74**, 2802–2808.

25 Jacobsen, T. K., Sorensen, B. F. and Brondsted, P. (1998) Measurement of uniform and localized heat dissipation induced by cyclic loading. *Exper. Mech.* **38**, 289–294.

26 Gamstedt, E. K., Redon, O. and Brondsted, P. (2002) Fatigue dissipation and failure in unidirectional and angle-ply glass fibre/carbon fibre hybrid laminates. *Exper. Tech. Design Compos. Mater. 5 Key Engng Mater* **221–2**, 35–47.